DEPARTMENT OF COMMERCE
UNITED STATES OF AMERICA

NOAA Technical Memorandum NESS 101

A COMPARISON OF SATELLITE OBSERVED MIDDLE CLOUD MOTION WITH GATE RAWINSONDE DATA

Washington, D.C.
January 1979

noaa NATIONAL OCEANIC AND ATMOSPHERIC ADMINISTRATION / National Environmental Satellite Service

NOAA TECHNICAL MEMORANDUMS

National Environmental Satellite Service Series

The National Environmental Satellite Service (NESS) is responsible for the establishment and operation of NOAA's environmental satellite systems.

NOAA Technical Memorandums facilitate rapid distribution of material that may be preliminary in nature and so may be published formally elsewhere at a later date. Publications 1 to 20 and 22 to 25 are in the earlier ESSA National Environmental Satellite Center Technical Memorandum (NESCTM) series. The current NOAA Technical Memorandum NESS series includes 21, 26, and subsequent issuances.

Publications listed below are available from the National Technical Information Service, U.S. Department of Commerce, Sills Bldg., 5285 Port Royal Road, Springfield, VA 22161. Prices on request. Order by accession number (given in parentheses). Information on memorandums not listed below can be obtained from Environmental Data and Information Service (D822), 6009 Executive Boulevard, Rockville, MD 20852.

NESS 61 Potential Value of Earth Satellite Measurements to Oceanographic Research in the Southern Ocean. E. Paul McClain, January 1975, 18 pp. (COM-75-10479/AS)

NESS 62 A Comparison of Infrared Imagery and Video Pictures in the Estimation of Daily Rainfall From Satellite Data. Walton A. Follansbee and Vincent J. Oliver, January 1975, 14 pp. (COM-75-10435/AS)

NESS 63 Snow Depth and Snow Extent Using VHRR Data From the NOAA-2 Satellite. David F. McGinnis, Jr., John A. Pritchard, and Donald R. Wiesnet, February 1975, 10 pp. (COM-75-10482/AS)

NESS 64 Central Processing and Analysis of Geostationary Satellite Data. Charles F. Bristor (Editor), March 1975, 155 pp. (COM-75-10853/AS)

NESS 65 Geographical Relations Between a Satellite and a Point Viewed Perpendicular to the Satellite Velocity Vector (Side Scan). Irwin Ruff and Arnold Gruber, March 1975, 14 pp. (COM-75-10678/AS)

NESS 66 A Summary of the Radiometric Technology Model of the Ocean Surface in the Microwave Region. John C. Alishouse, March 1975, 24 pp. (COM-75-10849/AS)

NESS 67 Data Collection System Geostationary Operational Environmental Satellite: Preliminary Report. Merle L. Nelson, March 1975, 48 pp. (COM-75-10679/AS)

NESS 68 Atlantic Tropical Cyclone Classifications for 1974. Donald C. Gaby, Donald R. Cochran, James B. Lushine, Samuel C. Pearce, Arthur C. Pike, and Kenneth O. Poteat, April 1975, 6 pp. (COM-75-1676/AS)

NESS 69 Publications and Final Reports on Contracts and Grants, NESS-1974. April 1975, 7 pp. (COM-75-10850/AS)

NESS 70 Dependence of VTPR Transmittance Profiles and Observed Radiances on Spectral Line Shape Parameters. Charles Braun, July 1975, 17 pp. (COM-75-11234/AS)

NESS 71 Nimbus-5 Sounder Data Processing System, Part II: Results. W. L. Smith, H. M. Woolf, C. M. Hayden, and W. C. Shen. July 1975, 102 pp. (COM-75-11334/AS)

NESS 72 Radiation Budget Data From the Meteorological Satellites, ITOS 1 and NOAA 1. Donald H. Flanders and William L. Smith, August 1975, 22 pp. (PB-246-877/AS)

NESS 73 Operational Processing of Solar Proton Monitor Data. Stanley R. Brown, September 1975. (Revision of NOAA TM NESS 49), 15 pp. (COM-73-11941)

NESS 74 Monthly Winter Snowline Variation in the Northern Hemisphere from Satellite Records, 1966-75. Donald R. Wiesnet and Michael Matson, November 1975, 21 pp. (PB-248-437)

NESS 75 Atlantic Tropical and Subtropical Cyclone Classifications for 1975. D. C. Gaby, J. B. Lushine, B. M. Mayfield, S. C. Pearce, and K. O. Poteat, March, 1976, 14 pp. (PB-253-968/AS)

NESS 76 The Use of the Radiosonde in Deriving Temperature Soundings From the Nimbus and NOAA Satellite Data. Christopher M. Hayden, April 1976, 21 pp. (PB-256-755)

NESS 77 Algorithm for Correcting the VHRR Imagery for Geometric Distortions Due to the Earth's Curvature and Rotation. Richard Legeckis and John Pritchard, April 1976, 30 pp. (PB-258-027/AS)

(Continued on inside back cover)

NOAA Technical Memorandum NESS 101

A COMPARISON OF SATELLITE OBSERVED MIDDLE CLOUD MOTION WITH GATE RAWINSONDE DATA

Leroy D. Herman

Washington, D.C.
January 1979

UNITED STATES
DEPARTMENT OF COMMERCE
Juanita M. Kreps, Secretary

NATIONAL OCEANIC AND
ATMOSPHERIC ADMINISTRATION
Richard A. Frank, Administrator

National Environmental
Satellite Service
David S. Johnson, Director

CONTENTS

A COMPARISON OF SATELLITE OBSERVED MIDDLE CLOUD MOTION WITH GATE RAWINSONDE DATA

Leroy D. Herman
National Environmental Satellite Service, NOAA
Washington, D. C.

ABSTRACT. Satellite middle cloud vectors were compared with GATE rawinsondes to determine their accuracy and altitudes. A method was derived for the estimation of middle level vector heights from satellite temperatures. The average vector deviation of satellite vectors from corresponding balloon winds at the estimated altitudes was 9.6 kt.

1. INTRODUCTION

Cloud motion vectors measured from geostationary satellite pictures approximate the wind at cloud altitude. Because of this correspondence these vectors are used in operational wind analyses in regions of sparse conventional wind data. The vectors are produced by the National Environmental Satellite Service (NESS) by two methods: (a) manual tracking of clouds in satellite movies as described by Young, Doolittle, and Mace (1972); and (b) computer matching of clouds from two pictures as described by Leese, Novak, and Clark (1971).

Most of the cloud motions measured by NESS are obtained for either high clouds or low clouds. Few observations of cloud motion are made in the middle levels -- 800 to 400 mb -- leaving a gap in the information needed for weather analysis. Many surface observations indicate that middle clouds occur fairly frequently, but these clouds are not being tracked by present methods.

The purpose of this study was to determine how well the height of middle cloud motions can be estimated from satellite observations. Cloud vectors were obtained from satellite observations during the GARP Atlantic Tropical Experiment (GATE) in the summer of 1974. Satellite-observed cloud displacements during Phase 2 (July 28 to August 16) were compared with nearby rawinsonde data from the GATE ship network. Only cloud motions that matched rawinsonde winds in the middle troposphere (800 to 400 mb) were investigated.

The apparent infrared cloud temperature as measured by the satellite radiometer, and the air temperature at the same altitude as measured by the radiosonde, may not agree. This occurs because the cloud elements may not completely fill the field of view of the radiometer, or the cloud may be partially transparent to radiation from lower levels. The relation between apparent cloud temperature, radiosonde temperature, and temperature of the underlying surface determines a quantity designated effective emissivity (ε). This quantity, which is also a function of radiometer field of view and element size, is discussed in section 2. Effective emissivity together with other cloud characteristics, such as cloud size and visible brightness, were examined for utility in judging altitudes.

2. DATA AND ANALYSIS PROCEDURE

Data used in this study were radiosondes in the GATE area centered on the A/B scale grid, and satellite data from SMS-1. Rawinsonde data at 1200 GMT during Phase 2 were obtained from the "quick look" tapes for locations shown in figure 1. Animated satellite picture sequences in both the visible and infrared, covering a 2-hour period centered at the time of the rawinsondes, were used to measure cloud motion. After editing unsuitable and doubtful data, 12 days from Phase 2 were analyzed.

The satellite cloud motion vectors were compared with the corresponding GATE rawinsonde observations. These cloud vectors were determined by tracking cloud targets within 180 n.mi. of the radiosonde positions. Each of these vectors was compared with its corresponding radiosonde winds to find the level of best fit (LBF). The LBF is the pressure level at which the sounding wind vector deviates the least from the cloud vector. It is the most likely level of cloud in the case of layer clouds.

Figure 2 is an example of the comparison of a sounding with a cloud motion vector. It shows the hodograph of the winds at Nouadhibou and the corresponding cloud motion vector at an LBF of 525 mb. Direction and vector deviations between cloud vector and balloon winds were computed for each cloud vector.

Comparisons were not used where the direction deviation at all levels was greater than 50° or the vector deviation at all levels was greater than the cloud motion speed. Cases were also discarded if there were multiple LBFs or if the minimum vector deviations at all levels were larger than 10 kt.

Cloud targets of doubtful reliability were not tracked. Early in the study we found that many middle cloud motions are not reliable indicators of advective motion. Effects such as development or evaporation simulate motion that did not correspond to any observed wind, and the animated sequences often showed gravity waves causing cloud propagation.

After locating the LBF, the sounding temperature at that altitude was taken to be the temperature of the cloud. The LBF temperature, the apparent cloud temperature measured from the satellite, and the surface temperature, are related by the effective emissivity as follows:

$$\varepsilon = \frac{B(T_{sfc}) - B(T_{sat})}{B(T_{sfc}) - B(T_{LBF})} \qquad (1)$$

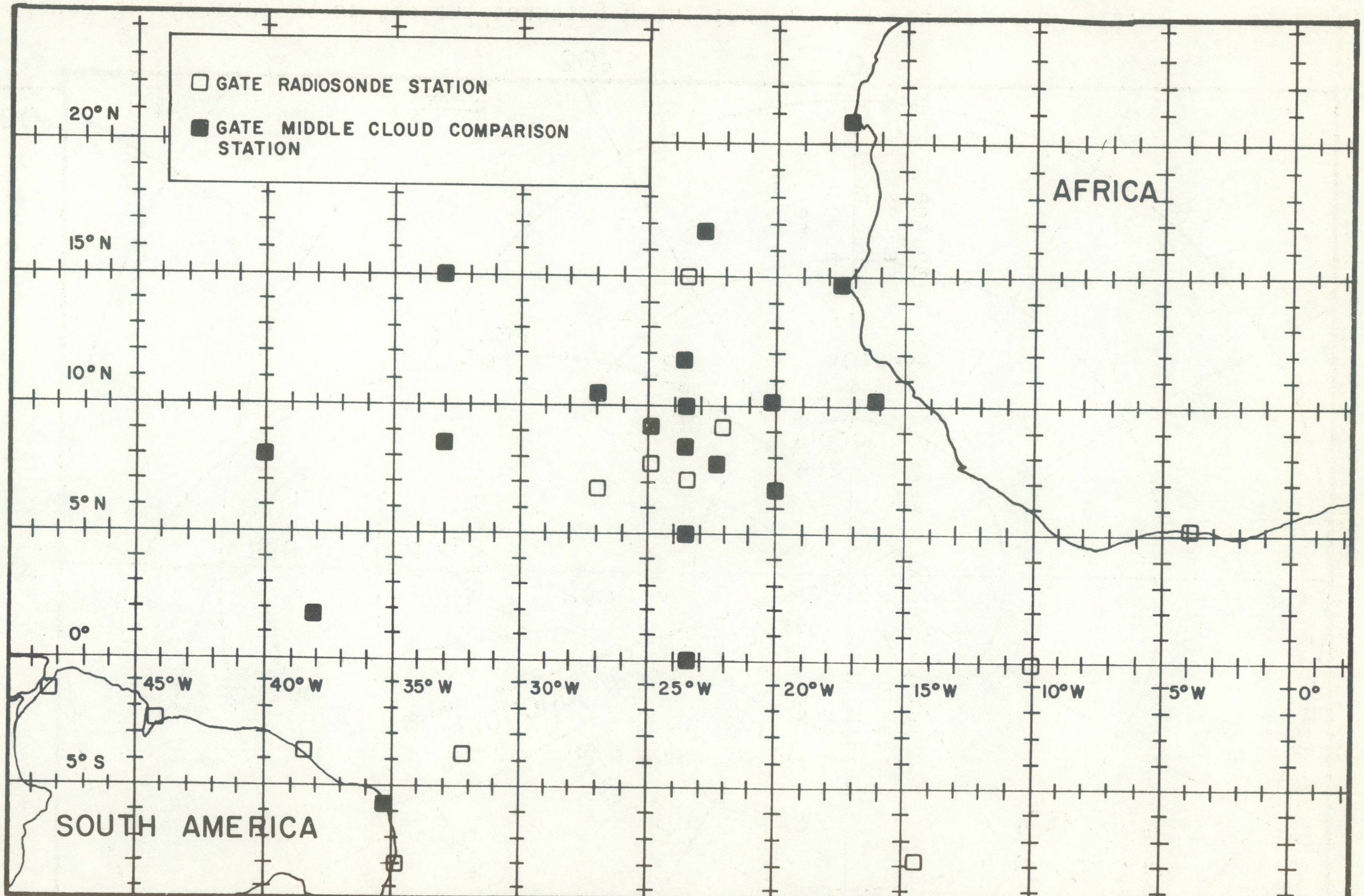

Figure 1.--GATE rawinsonde network during Phase 2 (July 28-August 16, 1974). The darkened boxes indicate stations where comparisons were made with middle clouds.

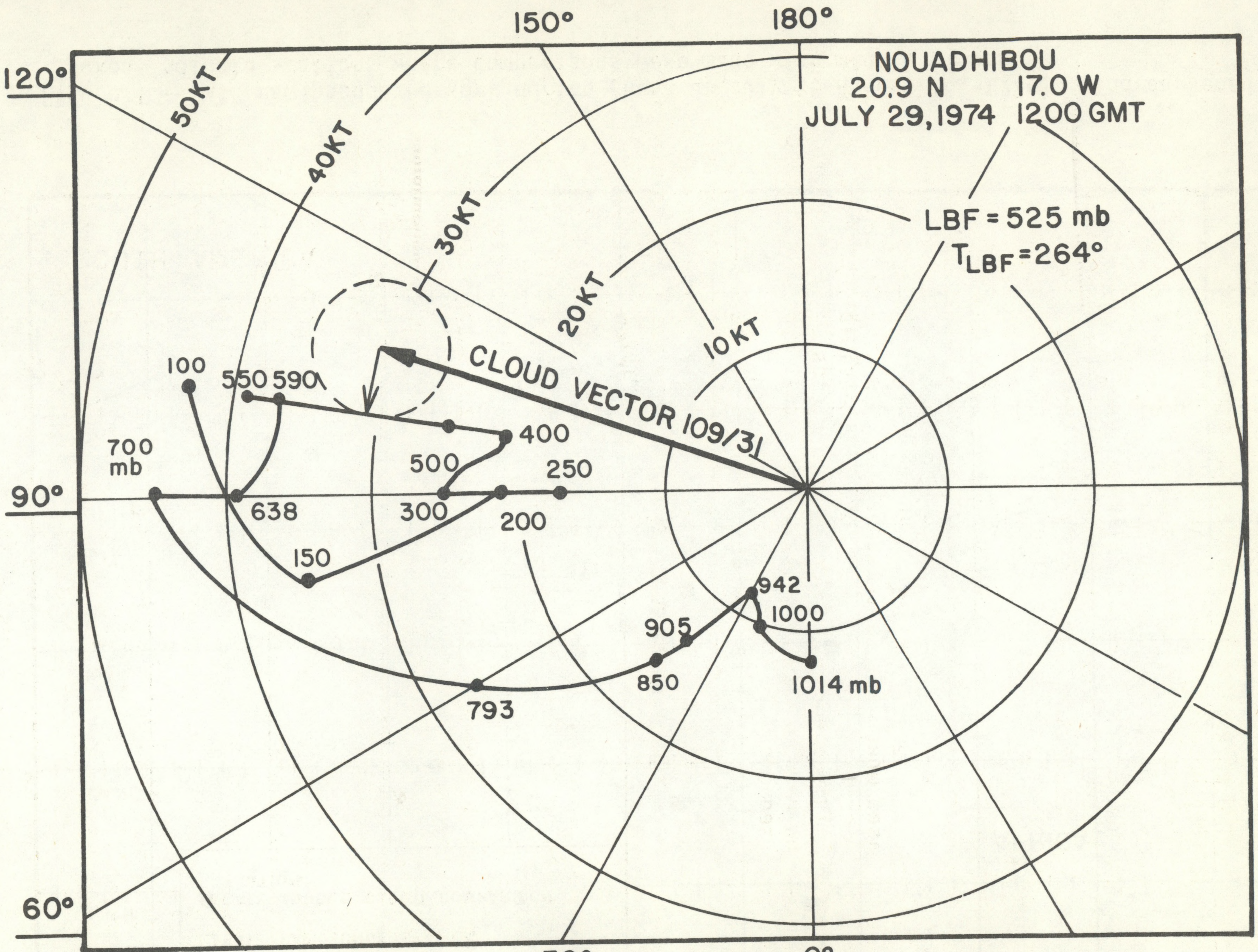

Figure 2.--Comparison of typical sounding with cloud motion vector. LBF (level of best fit) determined from minimum deviation circle.

where ε is the effective emissivity, T_{sat} is the cloud temperature measured by the satellite, T_{sfc} is the temperature of the underlying surface, T_{LBF} is the LBF temperature, and the B terms are the radiances at the specified temperatures. The effective emissivity used here is not the commonly defined emissivity because it is influenced by the sensor field of view relative to the cloud element size and cloud thickness.

Normally one would expect to find ε to be less than unity, which is the case when the apparent cloud temperature measured by the satellite is higher than the temperature at the LBF taken from the sounding. While a value of ε greater than unity is not physically possible, such values can result from the equation. This occurs when the cloud moves at a speed corresponding to the wind at a lower (warmer) level instead of the wind at the cloud top. This is most likely to occur with convective clouds.

The cloud targets were tracked from the infrared pictures for the most part, but in cases where the contrast between the cloud and background was too small to be certain of the cloud motion, the visible picture sequence was also used. This occurred primarily with fields of small cumulus clouds. Occasionally low emissivity clouds at other levels could be tracked better in the visible sequence.

Problems affecting the accuracy of comparisons between rawinsondes and cloud vectors were discussed by Hubert and Timchalk (1972) and Hasler et al. (1976). In the present study, special care was taken to minimize the errors of cloud target selection by applying the following restrictions:

a. The same cloud must be seen on each frame in the sequence. The formation or flickering of a cloud during the sequence disqualifies it.

b. The cloud must remain about the same size, shape, and temperature.

c. The erosion of a cloud band edge disqualifies it.

d. Clouds that significantly change direction or speed are disqualified.

e. The cloud must be representative of motions in the vicinity; at least one other similar cloud must display the same motion.

In addition, it is safest to choose middle cloud motions in areas where the high cloud motion is known or can be deduced from differential motions.

In order to apply these rules all variations in brightness, temperature, and other significant variables must be observed in detail. Two methods of enhancing picture detail were used. One way was to enlarge the pictures almost to the point where cloud element definition was lost. The other was to use half-mile resolution visible pictures when available. This higher resolution usually permitted the detection of previously unnoticed features and allowed better discrimination of relative cloud heights.

3. RESULTS

The number of clouds tracked for each of the 12 days is shown in table 1. While 380 clouds of all types were tracked and their motions compared with radiosonde winds, the right-hand column shows that only 38 had LBFs in the middle levels. Study of these middle clouds led to their division into three classes according to their emissivities and inferred vertical extent.

Class 1 middle clouds have effective emissivities less than unity. Table 2 shows that the LBF temperature of these clouds ranges from 256^{o} to 283^{o}K. However, because of their low effective emissivity the satellite temperatures range from $262^{o}$to 292^{o}K. These clouds are of primary interest because they probably occur in a single layer. The average vector deviation between the cloud motion and the wind at the LBF was only 4 kt.

Class 2 middle clouds have effective emissivities greater than unity. As mentioned earlier, this results from equation (1) only because each cloud top temperature is colder than its LBF temperature, as shown in table 3. This indicates that these clouds had motions associated with some level within the cloud. It implies that vertical development, probably convective in nature, influenced the cloud motion. None of the class 2 cloud tops, as indicated by the satellite temperature, were above middle levels. The LBF temperature ranged from 270^{o} to 287^{o}K, and the temperature of the tops ranged from 259^{o} to 282^{o}K (approximately 420 to 720 mb).

The class 3 middle clouds have LBFs in the middle level but are developed vertically with tops extending above the 400-mb level. The 11 clouds in this class, shown in table 4, also had effective emissivities greater than unity because their LBF temperatures (258^{o} to 283^{o}K) were much warmer than their apparent temperatures (213^{o} to 254^{o}K). Clouds with tops as cold as these look like high clouds. They would not ordinarily be recognized as potential middle cloud targets.

Of the three classes, clouds in class 1 are the most likely to provide the best targets for tracking because layer clouds are more nearly passive tracers that can be advected by the wind. Class 2 clouds are less useful middle level targets due to problems of estimating their altitude not found with the other two classes. However, because their tops are clearly in the middle layers, these clouds must be considered as potential cloud targets. Class 3 is of little interest here because the cold tops indicate vertical development to high altitudes, and when seen in a satellite picture could not be identified as middle cloud targets. Hence, class 3 was eliminated from further consideration.

Several cloud characteristics were considered as possible discriminators between classes 1 and 2. These included size, visible brightness relative to apparent temperature, and apparent temperature alone. The means of the cloud sizes of the two classes were subjected to a student t test which showed that their differences were not statistically significant. Therefore, size is not a discriminator. Visible brightness was then compared with apparent temperature. This was done by subjectively categorizing

Table 1.--Cloud motion vectors close to a radiosonde station

Date	Number of cloud vectors	Number of middle cloud vectors
7-29	28	3
7-31	29	4
8-01	24	3
8-02	26	4
8-03	35	3
8-05	36	2
8-09	50	2
8-10	34	2
8-12	31	2
8-13	37	8
8-14	28	2
8-16	22	3
	380 Total	38 Total

Table 2.--Class 1 - Single layer clouds with effective emissivities less than unity

Date	Cloud #	T_{LBF}	T_{sat}	Station	LBF pressure	LBF vector deviation	ε
		°K	°K		mb	kt	
7-29	8	264	269	61415	525	5	.87
7-31	19	265	274	EREU	500	10	.66
7-31	21	265	272	UMFW	478	7	.73
8-01	26	266	275	EREU	489	2	.59
8-02	1	269	286	GTUC	523	1	.24
8-03	32	266	272	DBBH	478	1	.78
8-03	38	283	283	UBLF	700	2	.95
8-09	5	261	267	EREB	441	1	.84
8-10	10	260	262	UHQS	427	6	.96
8-12	2	272	274	PWQO	564	4	.94
8-13	5	256	262	UHQS	400	0	.88
8-16	4	265	276	EREI	488	7	.69
8-16	10	279	287	GTUC	652	1	.59
8-16	16	282	292	PXSA	720	5	.42

Table 3.--Class 2 - Clouds with vertical development, bases and tops in the middle level

Date	Cloud #	T_{LBF}	T_{sat}	Station	LBF pressure	LBF vector deviation	T_{sat} pressure
		^oK	^oK		mb	kt	mb
7-29	9	286	259	61641	733	9	422
7-31	2	284	282	EREB	779	6	721
8-02	12	280	264	UPUI	668	4	465
8-02	16	283	269	UMFW	746	3	521
8-02	22	270	264	EREB	567	4	489
8-03	34	276	268	UMFW	635	6	508
8-05	2	287	281	EREH	794	1	669
8-05	10	280	274	DBBH	665	0	590
8-09	19	280	272	WEWP	668	1	553
8-10	14	279	264	UPUI	668	3	473
8-12	17	282	262	ERES	683	1	466
8-13	14	273	263	EREH	606	6	484
8-13	16	278	268	MVAN	662	7	520

Table 4.--Class 3 - Clouds with vertical development, bases in the middle level, and tops in the high level

Date	Cloud #	T_{LBF}	T_{sat}	Station	LBF pressure	LBF vector deviation	T_{sat} pressure
		^oK	^oK		mb	kt	mb
7-29	11	268	248	ERES	529	3	350
7-31	10	259	244	UPUI	419	1	300
8-01	12	264	233	GUDU	440	1	257
8-01	16	263	254	UMFW	431	7	361
8-13	7	273	237	EREH	606	4	282
8-13	10	263	249	08594	540	2	343
8-13	13	261	213	UHQS	500	1	171
8-13	15	276	245	MVAN	645	1	324
8-13	31	258	239	82599	422	2	300
8-14	7	271	242	UHQS	762	5	303
8-14	10	283	218	61641	719	2	197

each cloud as either gray or white in the visible and infrared, and partitioning each class separately into a four-way contingency table. Comparison of these tables showed the distributions were too similar to distinguish between the classes.

Consideration of the apparent infrared temperature as a discriminator proved more successful. The mean infrared temperatures of classes 1 and 2 differed by $6.6^{o}K$, which was statistically significant at the 5-percent level. As a first approximation the apparent temperature is a discriminator between these two classes with the threshold between them being at about $271^{o}K$.

The relation between the apparent infrared temperature, T_{sat}, and the temperature at the level of best fit of the class 1 data is shown in figure 3. The linear regression line relating these two variables is:

$$T_{LBF} \quad 50.47 + .7911\, T_{sat} \tag{2}$$

Here the correlation coefficient is 0.88. A similar linear regression line was calculated for the class 2 data. However, its low correlation of 0.40 indicates that the relation is too weak to be useful.

In summary, classes 1 and 2 contain cases of clouds whose motions are representative of middle levels. Although the sample is small and conclusions must be tentative, it appears that one should seek targets from clouds that have apparent temperatures ranging between 259^{o} and $292^{o}K$. The average pressure at the LBF for these two classes combined is 604 mb.

Three methods were tested for estimating the height of the vectors contained in classes 1 and 2:

(a) Assign the height to the mean pressure of all data in classes 1 and 2, viz. 604 mb.

(b) Assign the height to the pressure level where the apparent satellite temperature equals the air temperature.

(c) Assign the height to the level calculated from regression equation (2) for apparent temperatures greater than $271^{o}K$, and use method (b) for colder temperatures.

The average vector deviations between cloud vector and balloon wind were 11.9, 10.1, and 9.6 kt for the three methods (a), (b), and (c) respectively. The cumulative percentage frequencies of the vector deviations for these three methods shown in figure 4 indicates that the deviations of (c) are consistently smaller than (a) or (b). Student t tests based on the deviation differences showed that only the combination method (c) was significantly different from method (b) at the 5-percent level. Thus for the data in this sample the height of middle cloud can be determined better using method (c) than using the average middle level height.

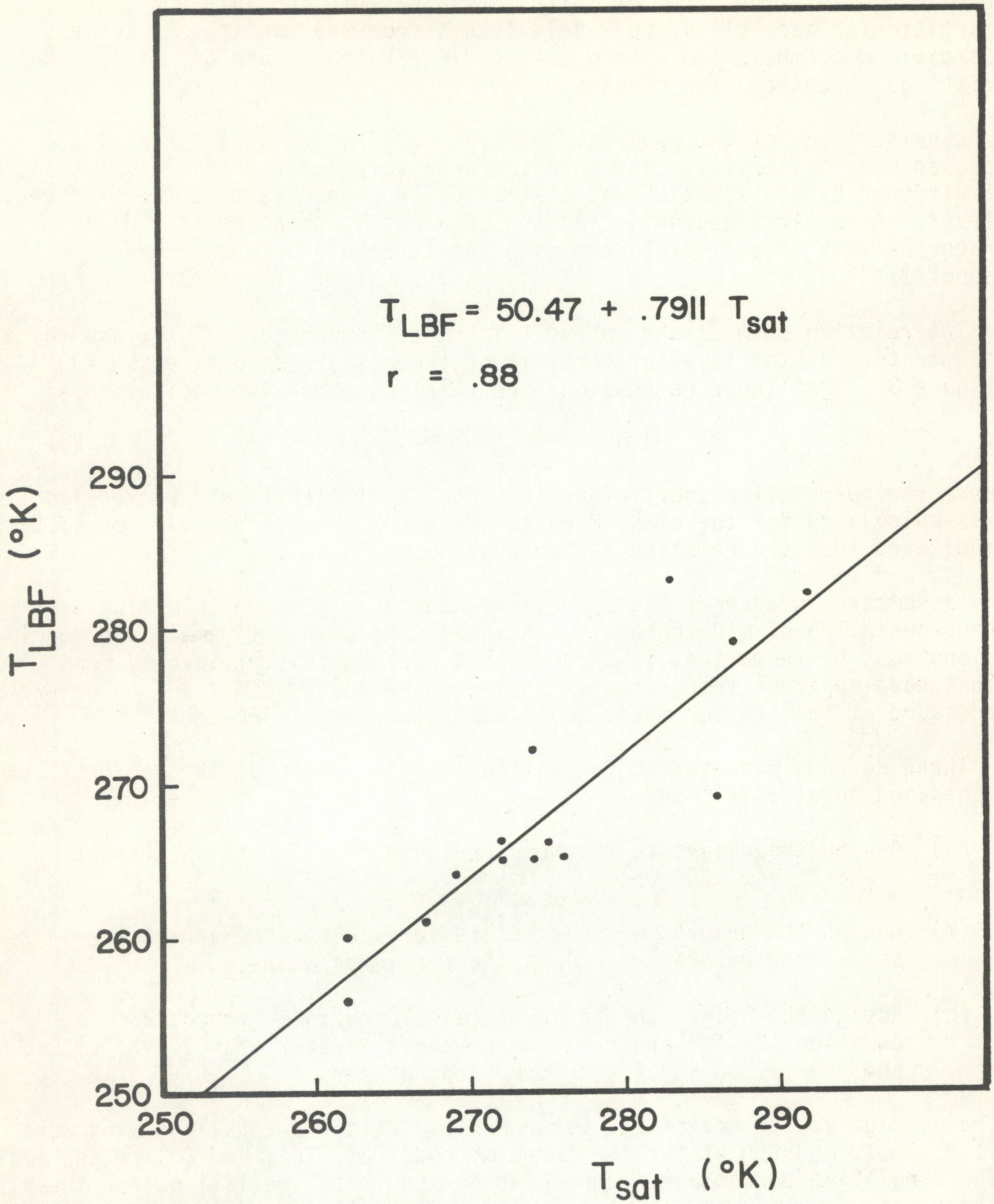

Figure 3.--Scatter diagram of the class 1 temperatures for 14 pairs of rawin and cloud vectors from Phase 2 of GATE.

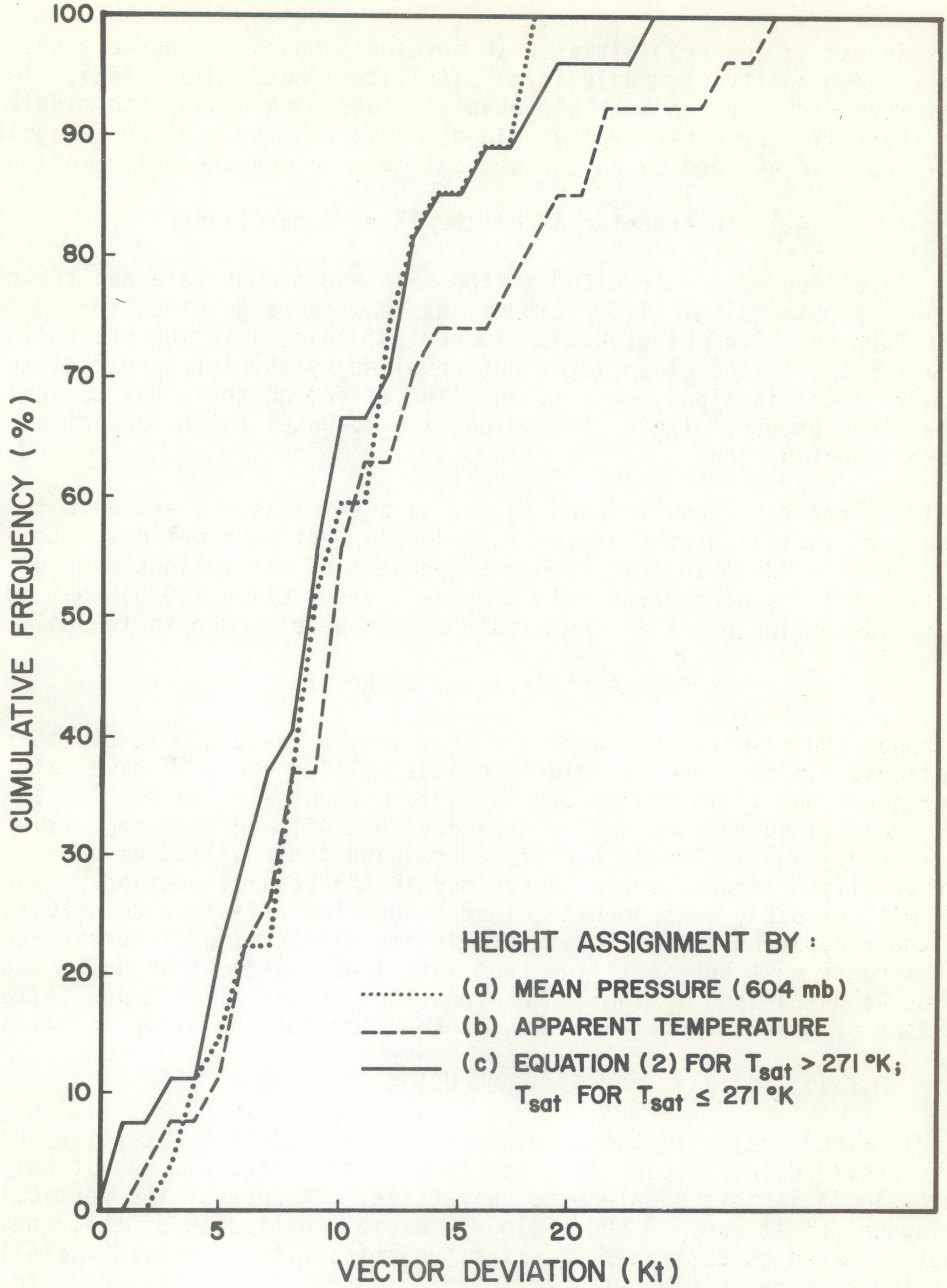

Figure 4.--Cumulative frequencies of vector deviation from LBF for heights assigned according to: (a) mean pressure, (b) apparent temperature, and (c) regression equation (2) for apparent temperatures warmer than 271°K, and apparent temperatures for colder values.

4. DISCUSSION

This investigation was initiated to develop a means to increase the quality and quantity of middle level satellite winds. Many middle clouds do not move with the wind; this probably occurs more often with middle cloud than with any other type of cloud. This problem must be recognized and if possible avoided by anyone who attempts to measure their motion.

4.1 Interpretation of the Three Data Classes

The comparison of middle cloud motion with radiosonde data has shown that the class 1 data, single layer clouds, has a wide range of ε, from a maximum of 0.96 to a minimum of 0.24. Sources of this variation probably are partial breaks in the cloud layer not resolved by the infrared radiometer, and differences in cloud composition. The effect on the ε due to variations in the cloud droplet size distribution, ice-to-water ratio, and cloud type require investigation.

Another important result found in the data of classes 2 and 3 is that clouds with various depths of vertical development have motions matching the middle level winds. In this sample 63 percent of the motions were of this variety. This is consistent with Simpson's observation (1976) that convective clouds having bases in the middle levels were common in the GATE area.

4.2 Applicability of Results

Although the results are tentative they appear to be applicable to routine operations. In the tropics, middle clouds will be found to have satellite temperatures mostly in the middle range from about -15° to $+15^{\circ}$C. In that range, some cloud motions can be measured that will be representative of middle level winds. The method of determining their altitudes depends on their satellite temperature as described in the results section. However, there will probably be some high clouds whose low effective emissivities make their apparent temperatures fall in the middle cloud temperature range. These targets must be identified from additional information using such methods as comparison of the cloud appearance in the visible and infrared, detection of unusually high speeds, or knowledge of the synoptic situation.

5. CONCLUSIONS

Middle cloud motion in the tropics can be derived from satellite observations, provided proper care is taken in selecting targets. About half the middle clouds in this sample were convective. Because of the vertical development of so many of these clouds, useable estimates of their height cannot be based on estimates of effective emissivity. Instead, satellite cloud temperature is the best parameter for determining altitude. For temperatures less than 271°K, altitude is estimated from the cloud temperature; for higher temperatures, altitude is estimated from regression. Because of the small size of the sample, these conclusions must be regarded as tentative.

ACKNOWLEDGMENT

The author wishes to express his appreciation to Lester F. Hubert for his suggestions and encouragement during the research phase and for his comments during the preparation of the manuscript.

REFERENCES

Hasler, A. E., and W. Shenk and W. Skillman, 1976: Wind Estimates from Cloud Motions: Phase 1 of an in situ Aircraft Verification Experiment. Journal of Applied Meteorology, Vol. 15, No. 1, pp. 10-15.

Hubert, L. F., and L. F. Whitney, Jr., 1971: Wind Estimation from Geostationary-Satellite Pictures. Monthly Weather Review, Vol. 99, No. 9 pp. 665-672.

Hubert, Lester F., and Andrew Timchalk, 1972: Convective Clouds as Tracers of Air Motion. NOAA Technical Memorandum NESS 40, 12 pp.

Leese, John A., Charles S. Novak and V. Ray Taylor, 1970: The Determination of Cloud Pattern Motions from Geosynchronous Satellite Image Data. Pattern Recognition, Pergamon Press, Great Britain, Vol. 2, pp. 279-292.

Simpson, Joanne, 1976: The GATE Aircraft Program: A Personal View. Bulletin of the American Meteorological Society, Vol. 57, No. 1, pp. 27-30.

Young, Michael T., Russell C. Doolittle and Lee M. Mace, 1972: Operational Procedures for Estimating Wind Vectors from Geostationary Satellite Data. NOAA Technical Memorandum NESS 39, 19 pp.

(Continued from inside front cover)

NESS 78 Satellite Derived Sea-Surface Temperatures From NOAA Spacecraft. Robert L. Brower, Hilda S. Gohrband, William G. Pichel, T. L. Signore, and Charles C. Walton, June 1975, 74 pp. (PB-258-026/AS)

NESS 79 Publications and Final Reports on Contracts and Grants, 1975. NESS, June 1976, 18 pp. (PB-258-450/AS)

NESS 80 Satellite Images of Lake Erie Ice: January-March 1975. Michael C. McMillan and David Forsyth, June 1976, 15 pp. (PB-258-458/AS)

NESS 81 Estimation of Daily Precipitation Over China and the USSR Using Satellite Imagery. Walton A. Follansbee, September 1976, 37 pp. (PB-261-970/AS)

NESS 82 The GOES Data Collection System Platform Address Code. Wilfred E. Mazur, Jr., October 1976, 26 pp. (PB-261-968/AS)

NESS 83 River Basin Snow Mapping at the National Environmental Satellite Service. Stanley R. Schneider, Donald R. Wiesnet, and Michael C. McMillan, November, 1976, 27 pp. (PB-263-816)

NESS 84 Winter Snow-Cover Maps of North America and Eurasia From Satellite Records, 1966-1976. Michael Matson, March 1977, 28 pp. (PB-267-393)

NESS 85 A Relationship Between Weakening of Tropical Cyclone Cloud Patterns and Lessening of Wind Speed. James B. Lushine, March 1977, 12 pp. (PB-267-392)

NESS 86 A Scheme for Estimating Convective Rainfall From Satellite Imagery. Roderick A. Scofield and Vincent J. Oliver, April 1977, 47 pp. (PB-270-762)

NESS 87 Atlantic Tropical and Subtropical Cyclone Classifications for 1976. D. C. Gaby, J. B. Lushine, B. M. Mayfield, S. C. Pearce, K. O. Poteat, and F. E. Torres, May, 1977, 13 pp. (PB-269-674)

NESS 88 NOAA CATALOG OF Products. Dennis C. Dismachek, Editor. June 1977, 120 pp. (PB-271-315)

NESS 89 A Laser Method of Observing Surface Pressure and Pressure-Altitude and Temperature Profiles of the Troposphere From Satellites. William L. Smith and C. M. R. Platt, July 1977, 38 pp. (PB-272-660)

NESS 90 Lake Erie Ice: Winter 1975-76. Jenifer H. Wartha, August 1977, 68 pp. (PB-276-386)

NESS 91 (In-Orbit Storage of NOAA/NESS Stand-by Satellites. Bruce Sharts, September 1977, 3 pp. (PB-283-078)

NESS 92 Publications and Final Reports on Contracts and Grants, NESS - 1976. Catherine M. Frain, Compiler, August 1977, 11 pp. (PB-273-169)

NESS 93 Computations of Solar Insolation at Boulder, Colorado. Joseph H. Pope, September 1977, 13 pp. (PB-273-679)

NESS 94 A Report on the Chesapeake Bay Region Nowcasting Experiment. Roderick A. Scofield and Carl E. Weiss, December 1977, 52 pp. (PB-277-102)

NESS 95 The TIROS-N/NOAA A-G Satellite Series. Arthur Schwalb, March 1978, 75 pp. (PB-283-859)

NESS 96 Satellite Data Set for Solar Incoming Radiation Studies. J. Dan Tarpley, Stanley R. Schneider, J. Emmett Bragg, and Marshall P. Waters, III, May 1978, 45 pp. (PB-284-740)

NESS 97 Publications and Final Reports on Contracts and Grants, 1977. Catherine M. Frain, compiler, August 1978.

NESS 98 Quantitative Measurements of Sea Surface Temperature at Several Locations Using the NOAA-3 Very High Resolution Radiometer. Laurence Breaker, Jack Klein, and Michael Pitts, August 1978.

NESS 99 An Empirical Model for Atmospheric Transmittance Functions and Its Applications to the NIMBUS-6 HIRS Experiment. P.G. Abel and W.L. Smith, NESS and A. Arking, NASA, September 1978.

NESS 100 Characteristics and Environmental Properties of Satellite-Observed Cloud Rows. Samuel K. Beckman, January 1979.

NOAA SCIENTIFIC AND TECHNICAL PUBLICATIONS

The National Oceanic and Atmospheric Administration was established as part of the Department of Commerce on October 3, 1970. The mission responsibilities of NOAA are to assess the socioeconomic impact of natural and technological changes in the environment and to monitor and predict the state of the solid Earth, the oceans and their living resources, the atmosphere, and the space environment of the Earth.

The major components of NOAA regularly produce various types of scientific and technical information in the following kinds of publications:

PROFESSIONAL PAPERS — Important definitive research results, major techniques, and special investigations.

CONTRACT AND GRANT REPORTS — Reports prepared by contractors or grantees under NOAA sponsorship.

ATLAS — Presentation of analyzed data generally in the form of maps showing distribution of rainfall, chemical and physical conditions of oceans and atmosphere, distribution of fishes and marine mammals, ionospheric conditions, etc.

TECHNICAL SERVICE PUBLICATIONS — Reports containing data, observations, instructions, etc. A partial listing includes data serials; prediction and outlook periodicals; technical manuals, training papers, planning reports, and information serials; and miscellaneous technical publications.

TECHNICAL REPORTS — Journal quality with extensive details, mathematical developments, or data listings.

TECHNICAL MEMORANDUMS — Reports of preliminary, partial, or negative research or technology results, interim instructions, and the like.

Information on availability of NOAA publications can be obtained from:

ENVIRONMENTAL SCIENCE INFORMATION CENTER (D822)
ENVIRONMENTAL DATA AND INFORMATION SERVICE
NATIONAL OCEANIC AND ATMOSPHERIC ADMINISTRATION
U.S. DEPARTMENT OF COMMERCE

6009 Executive Boulevard
Rockville, MD 20852

NOAA--S/T 78-136